Sensors and Actuators B 233 (2016) 314–319

Contents lists available at ScienceDirect

Sensors and Actuators B: Chemical

journal homepage: www.elsevier.com/locate/snb

Tailoring the sensing performances of an OFET-based biosensor

Stefano Lai[a,*], Massimo Barbaro[a], Annalisa Bonfiglio[a,b]

[a] Department of Electrical and Electronic Engineering, University of Cagliari, Piazza d'Armi, 09123, Cagliari, Italy
[b] CNR – Institute of Nanoscience, S3 Centre, Via Campi 213 A, 41125, Modena, Italy

ARTICLE INFO

Article history:
Received 27 October 2015
Received in revised form 19 March 2016
Accepted 18 April 2016
Available online 19 April 2016

Keywords:
DNA
Hybridization detection
OFET
bioFET
Sensors
Design

ABSTRACT

An approach for the fabrication of organic-FET based biosensors with precisely tailored sensing performances is here proposed. A specific device structure, namely Organic Charge-Modulated Field-Effect Transistor (OCMFET), has been analyzed in details and modeled in order to move beyond the pure phenomenological observation of its biochemical sensitivity and precisely determining its sensitivity. Thanks to a complete comprehension of the relationship between sensing ability and device structure, design rules have been derived for tailoring the sensing performances. The layout of the sensor has been optimized according to these design rules. The effectiveness of the approach and of the design is demonstrated by providing a complete electrical characterization of the device in a specific application, namely DNA hybridization detection. Record performances of the OCMFET for direct DNA hybridization detection, both in terms of sensitivity and selectivity, will be reported. As the sensing ability of the device is completely independent of the semiconductor employed for the transistor, the presented results are completely general and may be replicated also for other kinds of semiconductors, thus paving the way to a new generation of biosensing devices based on a variety of semiconducting materials.

© 2016 Elsevier B.V. All rights reserved.

1. Introduction

Since their first appearance in the late Seventies [1], biosensors based on Field-Effect Transistors, namely bioFETs, have been attracting a rising interest as valuable alternative to the standard instrumentation, mainly based on optical, biochemical and biophysical methods. BioFETs offer several advantages, including easy integration with electronic circuitries and, potentially, real-time, direct detection in a non-destructive manner. In the latest years, the employment of Organic FETs (OFETs) for the fabrication of bioFETs has been extensively investigated [2]. Complementary to standard silicon technologies, organic electronics offers several advantages in terms of low cost fabrication for large area processing, possibility of fabricating devices on flexible substrates and biocompatibility of the materials. So far, two main approaches have been proposed for the fabrication of organic bioFETs. In the first, the working principle of the Ion-Sensitive FET has been employed [3,4]. Such an approach, already successfully employed for several biochemical sensors in silicon technology [5–8], consists on the functionalization of the gate insulator with proper, electrically-charged biochemical receptors. If the investigated biochemical reaction takes place, the charge of the receptor changes, thus affecting the flat-band voltage of the transistor. Another approach, originally proposed for organic bioFETs, is related to a direct functionalization of the semiconductor with the biochemical receptors. This strategy has been particularly investigated for DNA hybridization detection. DNA hybridization is a basic biochemical reactions for several kind of analysis in medical, pharmaceutical and forensic applications. Several examples of OFET-based DNA hybridization sensors, operating both in dry [9,10], and wet conditions [11], have been proposed, as well as for Electrolyte-Gated OFETs (EGOFETs, [12]).

Significant attempts for the demonstration of actual feasibility of organic bioFETs in real applications have been made. As regards DNA hybridization detection, single nucleotide polymorphism rejection was firstly demonstrated by Bao and co-workers, as well as low voltage operation [11]. Low power consumption is one of the most important merit figures of EGOFETs, which have been demonstrated feasible for applications including also protein detection [13]. Nevertheless, a full exploitation of organic bioFETs in operational environments can be considered substantially missing. Alternatively to the commonly debated limitations of bioFET structures, such as the need of an external reference electrode in ISFET-like devices, or the poor environmental stability of the organic semiconductors, technological drawbacks can be also invoked to justify such a limited diffusion.

* Corresponding author.
E-mail address: stefano.lai@diee.unica.it (S. Lai).

http://dx.doi.org/10.1016/j.snb.2016.04.095
0925-4005/© 2016 Elsevier B.V. All rights reserved.

For instance, in ISFET-like devices, the transistor structure and the sensor performances are intrinsically related, thus not allowing their independent optimization. Indeed, in this class of devices the sensing area coincides with channel area W × L (being W and L channel width and length respectively). This strongly impacts on the reachable sensitivity in ISFET-based biosensors, which is expressed by the well-known relationship

$$\frac{dV_{TH}}{dQ_S} = \frac{1}{C_{INS}}\frac{1}{WL} = \frac{1}{C_{INS}A_S} \quad (1)$$

where C_{INS} is the capacitance of the gate insulator and Q_S is the charge anchored onto it. For instance, an increase of the sensitivity can be obtained by reducing the gate capacitance or the sensing area, i.e. reducing channel width and/or channel length; on the other hand, this determines respectively an increase of the transistor operating voltages and, possibly, current reduction and short channel effects [14].

For devices in which the receptors are directly anchored on the organic semiconductor, their chemical structure strongly influences the final sensing performances as well as thickness and morphology of the semiconductor film. For instance, the device reported by Zhang et al. [9] differs from those reported in Kim et al. [10] only for the active layer thickness, but the device response to DNA hybridization in terms of output current variation is exactly the opposite. It is thus clearly evident that the derivation of a precise and general model for this family of devices is virtually impossible.

A successful employment of organic bioFETs in operational environments, possibly aiming at market-attractive applications, requires the demonstration of a precise control of the device performances and the derivation of models and design rules allowing a reliable fabrication of large numbers of devices with reproducible performances. Here, a thorough investigation of a dedicated device structure will be proposed, and the possibility of actually design an OFET-based bioFET with a predetermined detection ability will be presented. This device structure, named Organic Charge-Modulated FET (OCMFET), already demonstrated record performances for DNA hybridization detection in terms of sensitivity and selectivity [15]. The aim of this paper is to go beyond the pure phenomenological observation of the OCMFET sensing ability, in order to demonstrate that its performances can be precisely tuned by tailoring its layout. An accurate model for the complete derivation of a relationship between the device structure and its sensitivity will be presented, and precise design rules will be reported. In order to demonstrate the precise control of the OCMFET sensing performances allowed by the derived design rules, a sensor particularly designed for DNA hybridization detection in the sub-picomolar range will be reported. The demonstration of the effectiveness of the design will be demonstrated by providing a complete characterization of the device in terms of sensitivity and selectivity.

2. Materials and methods

2.1. Device working principle and modelling

The OCMFET is a floating gate OFET, biased through a capacitively-coupled control gate. A part of the floating gate is directly exposed to the measurement environment, thus working as sensing area. Therefore, as the sensing area is physically separated from the active layer of the transistor, degradation of the organic semiconductor due to the measurement environment is also prevented. Moreover, the effective performances in terms of sensitivity are not strongly reliant on the choice of the semiconductor, thus making this approach feasible in different technologies. Indeed, this working principle has been already demonstrated in several applications, both in organic [15–17] and CMOS [18] technologies. It is also noteworthy that, differently from ISFET-based devices, the OCMFET does not need a reference electrode in the measurement solution, as its working point is set by the control gate; this represent a major advantage in terms of easiness of fabrication and handling.

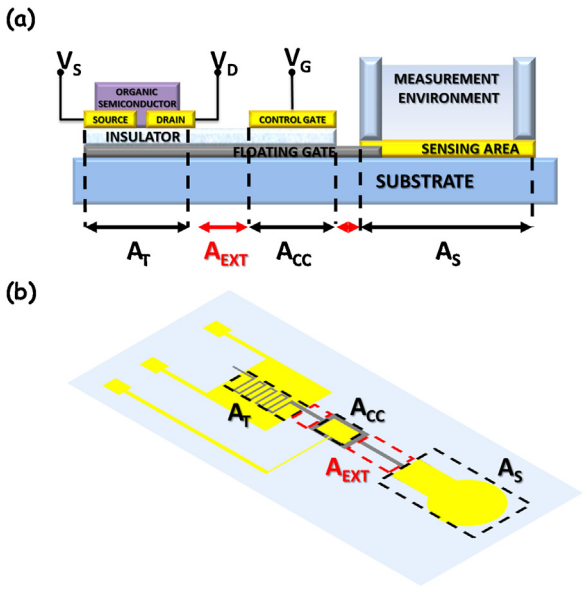

Fig. 1. (a) Section and (b) top view of the OCMET; in particular, the areas composing the floating gate are reported.

The device structure is reported in Fig. 1. The transduction mechanism of the OCMFET is the threshold voltage shift related to a charge variation occurring in the close proximity of the sensing area. For instance, by functionalizing the sensing area with single-stranded DNA sequences (probes), hybridization can be evaluated through the increase of the negative charge anchored onto the sensing area after the double-stranded DNA formation. As diffusely described in Barbaro et al. [19] and in Demelas et al. [20], the threshold voltage shift induced by a charge Q_S anchored onto the sensing area is

$$\Delta V_{TH} = -\frac{Q_S}{C_{SUM}} \quad (2)$$

being C_{SUM} the arithmetical sum of all the capacitances in the sensor layout, thus substantially including the control capacitance C_{CG} and all parasitic capacitances related to the transistor structure.

Such a simple model allows extrapolating the value of Q_S, but only partially describes the relationship between the OCMFET layout features and its actual sensitivity. Indeed, it takes into account only the capacitive structure of the sensor, while the amount of the charge Q_S actually transduced by the transistor also depends on the geometric dimensions of each element insisting on the floating gate. As depicted in Fig. 1, the total area of the floating gate, A_{TOT}, includes the transistor area (A_T), the control capacitor area (A_{CC}) and the sensing area (A_S); in addition, the connections between these elements (indicated as A_{EXT}) must be also taken into account. The charge Q_S anchored onto the sensing area induces a charge perturbation in the whole floating gate; if a perfect induction is considered, a charge $-Q_S$ is attracted in correspondence of the sensing area. Consequently, a charge $+Q_S$ is distributed among A_T, A_{CC} and A_{EXT} to maintain the charge conservation inside the floating gate. As only the charge lying in A_T, Q_T, is effective in the transduction, two first design rules can be derived: (i) the capacitance of the control gate should be significantly larger than the other ones in the layout in order to have a negligible charge variation in A_{CC}; (ii) as

the charge located in A_{EXT}, Q_{EXT}, is ineffective for transduction, such area should be minimized.

If the different areas are explicitly introduced in Eq. (2), the sensitivity can be written as

$$\left|\frac{dV_{TH}}{dQ_S}\right| = \frac{1}{C_{CG}+C_T} = \frac{1}{C_{INS}}\frac{1}{A_{CC}+(A_{OV}+WL)} = \frac{1}{C_{INS}}\frac{1}{A_{TOT}-A_S-A_{EXT}} \quad (3)$$

where the transistor area A_T is written as the sum of the channel area, $W \times L$ (being W and L the channel width and length, respectively) and the overlap area of source and drain with the floating gate, A_{OV}. The sum of A_{CC} and A_T can also be expressed as the difference between A_{TOT} and the other floating gate portions; by setting $A_S \gg A_{EXT}$, this last equation can be thus simplified in

$$\left|\frac{dV_{TH}}{dQ_S}\right| \approx \frac{1}{C_{INS}}\frac{1}{A_{TOT}-A_S} = \frac{1}{C_{INS}A_S}\frac{1}{A_{TOT}/A_S-1} \quad (4)$$

The last equation demonstrates that it is possible to finely tune the device sensitivity by properly choosing the value of the ratio between A_{TOT} and A_S: the larger A_S/A_{TOT}, the higher the final sensitivity. This means that the different areas composing the floating gate must be smaller than the sensing area; precise constraints on the device layout are thus introduced. Since A_S must be larger than $W \times L$, for a given dimension of the sensing area, the maximum value of the channel area is fixed. Secondly, as the control capacitor area must be kept small to increase A_S/A_{TOT}, it is also necessary to minimize the parasitic capacitances of the transistor, as they must be charged by the control gate to guarantee the proper biasing of the device.

It is noteworthy that the derived design rules demonstrate that, with respect to other bioFET structures, the OCMFET sensitivity depends on geometric features which can be tuned independently of the transistor channel area. For instance, the geometrical features of the transistor can be set according to the fabrication process and to the desired output current level; consequently, the control capacitor necessary to properly bias the device can be dimensioned, and finally the sensing area. As a matter of fact, the device electrical and sensing properties may be determined and optimized independently. This feature, added to the other already mentioned peculiarities of the device structure, makes the OCMFET approach uniquely attractive among bioFETs. In order to demonstrate the effectiveness of the derived design rules, an OCMFET-based sensor for DNA hybridization detection in the sub-picomolar range was designed, fabricated and tested.

2.2. Device fabrication

The devices here tested were fabricated onto a 175 μm-thick polyethylene terephthalate (PET) substrate (Goodfellow). The floating gate was patterned by means of photolithography on an aluminum film, deposited by thermal evaporation at 10^{-4} Torr. The aluminum surface was oxidized by storing the substrate in an oven at 50 °C for at least 12 h, obtaining an average thickness of the aluminum oxide of about 8 nm. A hybrid organic/inorganic insulating layer, acting as dielectric for both the transistor and the control capacitor, was obtained by depositing a 35 nm-thick Parylene C (Specialty Coating Systems) by means of Chemical Vapor Deposition (Labcoater 2 PDS 2010, Specialty Coating Systems). In order to reduce parasitic capacitances, self-alignment of source and drain electrodes with the floating gate was performed according to the technique reported in [21]. Self-alignment involved only the channel of the device thanks to a double-side development of the photoresist: the floating gate acted as mask for the UV light coming from the back side of the substrate, while a second mask was employed on the other side. In this way, the photoresist polymerized only on the channel area. After gold deposition by thermal evaporation (10^{-4} Torr), the lift-off of the gold coating the channel was performed by rinsing the substrate with acetone. Control gate and sensing area were finally patterned by means of photolithography. 6,13-Bis(triisopropylsilylethynyl)pentacene (TIPS Pentacene, Sigma-Aldrich) was employed as semiconductor. It was deposited by drop casting of a 0.5 wt% solution of TIPS Pentacene in toluene; crystallization of the semiconductor was improved by drying the device at 90 °C on a hot plate. All the biochemical procedures involving the sensing areas were carried out into incubation chambers fabricated in acrylic glass poly(methyl methacrylate) (PMMA) and mounted on the substrate. The device was finally encapsulated by means of a 2 μm-thick Parylene C layer and the transistor area was covered with a black tape in order to avoid any a-specific effect due to the photosensitivity of TIPS Pentacene.

2.3. Functionalization process

The DNA sensitivity of the OCMFET was obtained by anchoring single-stranded DNA probes onto the sensing area. The probe sequence is P = HS-5′-$(T)_{13}$- GGT TTC CGC CCC TTA GTG-3′. Before probe immobilization, the sensing area of the device was cleaned and sterilized with sodium hypochlorite. The functionalization of the sensing area with the DNA probes was performed by spotting a 100 nM solution of P in a 1 M potassium phosphate monobasic (KH_2PO_4, Sigma-Aldrich) buffer, from now on called the functionalization buffer. After two hours, a 1 mM solution of 6-mercapto-1-hexanol (MCH, Sigma-Aldrich) was spotted onto the sensing area; MCH molecules act as spacers and prevent the folding of the probes [22]. The device was then stored overnight in order to allow the self-alignment of the probes.

2.4. Hybridization process

Hybridization tests were performed at room temperature by spotting a solution of target sequences diluted in TE 1 M NaCl (10 mM Tris–HCl, 1 mM EDTA, 1 M NaCl, all reagents purchased by Sigma-Aldrich), from now on called the hybridization buffer. In this paper, three different target sequences were employed, all purchased by Sigma-Aldrich: a fully complementary target (T = 5′-CAC TAA GGG GCG GAA ACC-3′), a fully not-complementary target (U = 5′-AGAGCCTTTACACCGACT-3′) and a target sequence with a single nucleotide polymorphism (TSNP = 5′-CAC TAA GGG CCG GAA ACC-3′).

2.5. Measurement setup

All measurements were performed in liquid environment, in ambient conditions and at room temperature. A phosphate buffer solution (PBS, pH 7), with a 50 mM concentration of sodium chloride, was considered as measurement solution. Although this concentration is relatively high for bioFET operation, such a measurement buffer has been already successfully employed with OCMFET-based DNA sensors, thanks to its peculiar characteristics that made hybridization sensitivity less reliant on screening length conditions [23]. All the measurements have been performed using an Keithley® 2636 SourceMeter, controlled by custom-made Matlab® scripts. Each DNA hybridization sensor is composed by two OCMFETs: one is actually employed as sensor, while a second one is used as reference device, thus being exposed to the same measurement solution but without the DNA target strands. The sensitivity of the device is reported in terms of net threshold voltage shift, defined as the difference between the threshold voltage shift of a sensor after hybridization and that of the reference device. Thanks to such double-correlated differential approach, unspecific threshold voltage shift is compensated, thus being finally related only to the detected charge. The device selectivity was investigated by recording in real time the output current of the device during the hybridization process. A constant source-to-drain voltage drop

V_{DS} was set, while the control gate was biased with a square-wave voltage V_{GS} in order to reduce the bias stress effect of the organic transistor; indeed, this could lead to a continuous current reduction possibly masking the expected current increase related to the hybridization effect. The amplitude and the frequency of the voltage drop were chosen in order to make all the devices work in the same over-threshold conditions. The efficiency of the hybridization was evaluated by measuring the relative variation in the output current, $\Delta I_{DS}/I_{DS,baseline}$, where $I_{DS,baseline}$ is the output current before spotting the target sequences.

3. Results and discussion

3.1. Design of DNA hybridization sensor in the sub-picomolar range

DNA hybridization detection has been diffusely employed as testbench for characterizing the detection ability of bioFETs. So far, the lowest detection limit is of 100 fM for graphene-based bioFETs [24], using PNA probes for detection. For DNA probes, a detection limit of 1 pM has been obtained, as the electrostatic repulsion between probes and target sequences reduces hybridization efficiency [25]. Among organic-based bioFETs, the OCMFET reported in [15] has the better performances in terms of sensitivity to our knowledge, with a measured target concentration of 100 pM.

The optimized OCMFET in this paper was designed to reach a detection limit of 100 fM, thus making an organic-based bioFET competitive with graphene-based ones. As consistent reference for the optimized device dimensioning, the former implementation of the OCMFET reported in [15], fabricated with the same technology for low voltage devices, was considered; in particular the same insulating capacitance and the same sensing area dimensions have been employed ($C_{INS} = 74\ nF\,cm^{-2}$ and $A_S = 0.28\ cm^2$, respectively). In the former implementation, a charge of about 16 nC was detected at 100 pM target concentration. When the target DNA concentration goes in the femtomolar regime, a significant reduction of the surface coverage would be expected. Therefore, a lower charge would be anchored during hybridization: as rough starting point, $Q_S = 1\ nC$ was considered. At 100 fM detection limit, a net threshold voltage shift comparable to the noise level should be obtained; in the double-correlated differential mode, the maximum noise level is defined by the residual difference in the a-specific threshold voltage shift of sensor and reference devices. This a-specific shift has been evaluated as about 70 mV over a few tens of tested devices (see Supplementary materials). According to these constraints, a sensitivity of about $7 \times 10^7\ VC^{-1}$ should be obtained according to Eq. (4). Therefore, by inverting Eq. (4), a specific value of A_{TOT} can be derived,

$$A_{TOT} = A_S \left(\frac{1}{C_{INS} A_S} \left| \frac{dV_{TH}}{dQ_S} \right|^{-1} + 1 \right) = 0.43\ cm^2$$

This area should be mainly composed by the transistor area and the control capacitor area. A transistor area $A_T = W \times L = 1 \times 10^{-2}\ cm^2$ was chosen, thus being significantly smaller than A_S; for $L = 30\ \mu m$, a reasonable value for the available fabrication technology, a W of $3.3\ cm$ was dimensioned. Consequently, a total parasitic capacitances $C_P = 2 \times C_{INS} \times W \times L_{OV} = 93\ pF$ has been derived, being $L_{OV} = 2\ \mu m$ as evaluated for the self-alignment process reported in [21]. The control capacitor area was dimensioned to be at least two order of magnitudes larger than C_P; by sizing $A_{CC} = 0.18\ cm^2$, a control capacitance of $C_{CG} = 13.8\ nF$ was obtained. This control capacitance dimensions allowed making the external area significantly lower than all the other areas ($A_{EXT} = 3 \times 10^{-3}\ cm^2$). All the geometrical parameters have been reported in Table 1.

Table 1
Resume of the geometrical features of the OCMFET and theoretical sensitivity according to the design rules.

Parameter	Optimized layout
Sensing area (A_S) [cm^2]	0.28
Transistor area (A_T) [cm^2]	1×10^{-2}
Channel area ($W \times L$) [cm^2]	$3.3 \times (3 \times 10^{-3})$
Overlap area ($A_{SF} = A_{DF}$) [cm^2]	5.4×10^{-4}
Control capacitor area (A_{CC}) [cm^2]	0.18
External area (A_{EXT}) [cm^2]	3×10^{-3}
Total floating gate area (A_{TOT})[cm^2]	0.43
Gate capacitance (C_{INS}) [F cm^{-2}]	74×10^{-9}
Theoretical Sensitivity (dV_{TH}/dQ_S) [V C^{-1}]	$\mathbf{7 \times 10^7}$

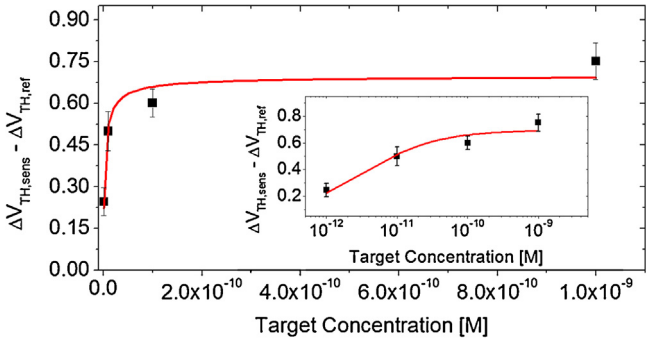

Fig. 2. Calibration curve of the OCMFET response to target concentration in solution. The response is in terms of net threshold voltage shift, i.e. the difference between the threshold voltage shift recorded in the sensor and the one recorded in a reference device. Threshold voltage shift have been evaluated from output characteristic curves of the device acquired before and after hybridization. Hybridization was performed in ambient conditions and at room temperature. In the inset, the same graph in semi-logarithmic scale is reported.

3.2. Sensitivity test and design validation

Sensitivity and selectivity of the optimized OCMFET to DNA hybridization are reported in Fig. 2 in terms of net threshold voltage shift (averaged on three samples per concentration), according to what described in Section 2.5. Calibration was performed by testing DNA hybridization with different concentrations of complementary target (T) sequences in the hybridization solution; according to the employed concentration, the hybridization time, i.e. the amount of time between the spotting of the target sequence and the measurement, varied from 90 min to 24 h. The device correctly responded in the range 1 nM–1 pM, with restrained error bars and net threshold voltage shifts significantly larger than the noise limit of 70 mV. Interestingly enough, the measured data fit the Sips isotherm absorption model, which is commonly used for multiple binding energy absorption of low concentrations of biomolecules over rough surfaces [26],

$$\frac{y}{Y_0} = \frac{kC^{1/m}}{1 + kC^{1/m}}$$

being Y_0, k and m the fitting parameters, which have been calculated by means of a custom Matlab® function ($Y_0 = 0.6984\ V$, $k = 10^9\ M^{-1}$ and $m = 1.2869$). The detection limit has been evaluated by inverting the previous equation to evaluate the concentration C_n corresponding to a net threshold voltage shift variation equal to the average noise limit of $y_n = 70\ mV$.

$$C_n = \left[\frac{y_n/Y_0}{k(1 - y_n/Y_0)} \right]^m = 155\ fM$$

Such value is the lowest detection limit ever reported for organic bioFETs, and substantially identical to those imposed in the layout design. The residual difference could be surely related to residual

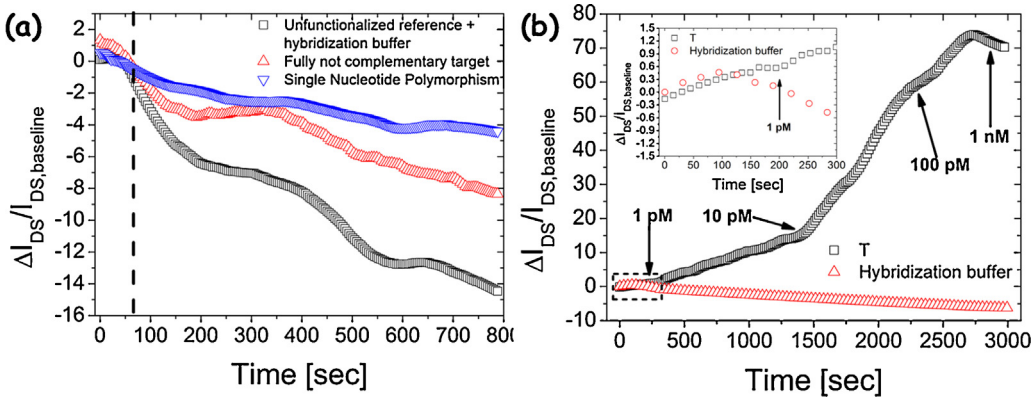

Fig. 3. Real time percentage current variation (ΔI_{DS}) of the OCMFET during hybridization tests, normalized to the baseline current ($I_{DS,baseline}$), that is the current recorded before the injection of target DNA strands. (a) False positive screening, performed by acquiring the response of the unfunctionalized reference to the hybridization buffer (squares), to fully not complementary target sequences (diamond) and to target sequences with SNP (circles). The analytes were inserted at T = 60 s; before this time, a part of the a-specific transient of the OCMFET device is reported. (b) Response of the sensor to fully complementary target sequences (squares) over a period of time of 3000s, compared to the response of a reference device functionalized with ssDNA probes to bare hybridization buffer (circles). In the inset, a magnification of the area in the dashed box is reported to show the a-specific dynamic and the initial response of the device to 1 pM target concentration. During the experiment, the target concentration was progressively increased, up to 1 nM.

measurement noise and to small differences in the functionalization and hybridization efficiency with respect to what considered during design. In any case, an almost perfect fitting of results with the expected performances could be considered achieved.

3.3. Selectivity test

In order to complete the evaluation of the device performances, selectivity tests were also performed with real time output current measurements, as described in Section 2.4. To investigate the reliability of the device detection ability, hybridization tests were carried out using fully complementary target sequences, fully not complementary target sequences and target molecules including a single nucleotide polymorphism (SNP) in the middle of the sequence. Moreover, the response of the reference (not functionalized) device in time was also evaluated. The results are reported in Fig. 3. False positive investigation is reported in Fig. 3(a). The dashed line represents the time when the different analytes where spotted on the sensing area. The reference device was measured in real time during exposure to the bare hybridization buffer: in this case, a significant reduction of the output current was recorded, and this can be ascribed to the residual bias stress, which is already visible before the hybridization buffer spotting. A similar trend was also observed in functionalized devices exposed both to fully not complementary and single-polymorphic target sequences with a 1 nM concentration. In these cases, the final amount of the current reduction is lower, probably related to intrinsic charge of floating not complementary sequences in the measurement solution or to a-specific hybridizations. Nevertheless, these effects resulted not sufficient to determine an overall increase of the output current.

In Fig. 3(b), the real-time current variation related to complementary target sequences is reported. In particular, target concentration was varied during the current acquisition from 1 pM to 1 nM. In the plot, a slight increase of current can be noticed even before the spotting of the target molecules at the concentration of 1 pM (at T = 200 s ca.): such a very slow and small variation can be related to a residual device dynamic, thus being a-specific. It is noteworthy that a similar trend can be noticed also in a reference device (i.e., a sensor functionalized with ssDNA exposed to bare hybridization buffer); in this device, a decrease of the output current in time, related to the bias stress effect, can be noticed. In the sensor, the dynamic started to change a few seconds after the target spotting, and the current started to increase in a more significant way. This almost immediate response have been already observed in the previous implementation of the OCMFET, and represent a figure merit of this approach. At the time the concentration was increased to 10 pM (after 20 min ca.), a current variation of about 15% was obtained. With the 10 pM concentration, the slope became more relevant, and, after about 15 min, the current variation reached the impressive value of 60%. This time was sufficient to almost completely saturate the device response: no significant variation in the dynamic of the response was noticed after a further increase of the target concentration to 100 pM. Moreover, after 2800 s, the current started to decrease. This can be related to a complete saturation of the anchored probes; after that, as no more increases in the output current can be induced, the bias stress become dominant in the transistor response. As a proof, further increases in the target concentration did not modify this trend, and the current continued to decrease.

A final current variation of about 75% was finally recorded; as the response to single nucleotide polymorphism is an overall reduction current of about 5% a noise margin of about 80% of the output current has been obtained. These noise margins are the highest reported for bioFETs, also improving the results reported for our previous implementation of the OCMFET. This increase of the selectivity can be ascribed to the smaller employable concentrations allowed by the enhanced device sensitivity: indeed, as hybridization of not fully complementary target molecules is very slow at low concentrations (if compared to those of fully complementary DNA strands), their effect in the transistor response is suddenly hidden by other effects related to the transistor structure, such as bias stress.

4. Conclusions

In this paper, the possibility of going beyond a pure phenomenological evaluation of the sensing performances of a specific organic bioFET device, namely OCMFET, by deriving actual design rules for tailoring its sensing performances has been reported. The developed model shows that, uniquely among bioFET structures, the OCMFET approach allows independently optimizing the transistor structure and the sensing performances of the device. This feature, here thoroughly analysed for the first time, is summed to other peculiar characteristics of the OCMFET approach, thus making this class of devices promising for several kinds of biochemical sensing applications. As an effective testbench for the proposed approach,

a DNA hybridization sensor particularly conceived for operating in the picomolar range, and with a nominal detection limit of 100 fM, was designed, fabricated and tested. The device was able to detect DNA hybridization for target concentrations as low as 1 pM, with an extrapolated detection limit of 155 fM, which is in good agreement with the initial design. The device also showed the capability of unambiguous recognition of SNP. The reported results define new record performances for organic bioFETs in terms of sensitivity and selectivity, and interestingly competitive with those so far reported for inorganic bioFETs and graphene-based devices.

Acknowledgments

S. Lai gratefully acknowledges Sardinia Regional Government for the financial support of his PhD scholarship (P.O.R. Sardegna F.S.E. Operational Programme of the Autonomous Region of Sardinia, European Social Fund 2007–2013 – Axis IV Human Resources, Objective l.3, Line of Activity l.3.1.)". The authors acknowledge Sardinia Regional Government for funding the activity in the scope of the project "BioFET" (L.R. 7/2007) and the Minister of University and Research for funding the activity in the scope of the project "MIND" (PRIN 2010–2011).

Appendix A. Supplementary data

Supplementary data associated with this article can be found, in the online version, at http://dx.doi.org/10.1016/j.snb.2016.04.095.

References

[1] J. Janata, S.D. Moss, Chemically sensitive field-effect transistors, Biomed. Eng. (N.Y.) 11 (1976) 241–245.
[2] P. Lin, F. Yan, Organic thin-film transistors for chemical and biological sensing, Adv. Mater. 24 (2012) 34–51.
[3] C. Bartic, A. Campitelli, S. Borgs, Field-effect detection of chemical species with hybrid organic/inorganic transistors, App. Phys. Lett. 82 (2003) 475–477.
[4] A. Loi, I. Manunza, A. Bonfiglio, Flexible, organic, ion-sensitive field-effect transistor, App. Phys. Lett. 86 (2005) 103512.
[5] J.F. Schenck, Technical difficulties remaining to the application of ISFET devices, in: P.W. Cheung (Ed.), Theory, Design and Biomedical Application of Solid State Chemical Sensors, CRC Press Inc., Boca Raton, 1978, pp. 165–173.
[6] S. Caras, J. Janata, Anal. Chem. 52 (1980) 1935–1937.
[7] E. Souteyrand, J.P. Cloarec, J.R. Martin, C. Wilson, I. Lawrence, S. Mikkelsen, M.F. Lawrence, J. Phys. Chem. B 101 (1997) 2980–2985.
[8] J.M. Rothberg, et al., An integrated semiconductor device enabling non-optical genome sequencing, Nature 457 (2011) 348–352.
[9] Q. Zhang, V. Subramanian, DNA hybridization detection with organic thin film transistors: toward fast and disposable DNA microarray chips, Biosens. Bioelectron. 22 (2007) 3182–3187.
[10] J.-M. Kim, S.K. Jha, R. Chand, D.-H. Lee, Y.-S. Kim, DNA hybridization sensor based on pentacene thin film transistor, Biosens. Bioelectron. 26 (2011) 2264–2269.
[11] H.U. Khan, M.E. Roberts, O. Johnson, R. Förch, W. Knoll, Z. Bao, In situ, label-free DNA detection using organic transistor sensors, Adv. Mater. 22 (2010) 4452–4456.
[12] L. Kergoat, B. Piro, M. Berggren, M.-C. Pham, A. Yassar, G. Horowitz, DNA detection with a water-gated organic field-effect transistor, Org. Electron. 13 (2012) 1–6.
[13] M.Y. Mulla, P. Seshadri, L. Torsi, K. Manoli, A. Mallardi, N. Ditaranto, M.V. Santacroce, C. Di Franco, G. Scamarcio, M. Magliulo, UV crosslinked poly(acrylic acid): a simple method to bio-functionalize electrolyte-gated OFET biosensors, J. Mater. Chem. B 3 (2015) 5049–5057.
[14] Y. Chen, I. Shih, Scaling down of organic thin film transistors: short channel effects and channel length-dependent field effect mobility, J. Mater. Sci. 44 (2009) 280–284.
[15] S. Lai, M. Demelas, G. Casula, P. Cosseddu, M. Barbaro, A. Bonfiglio, Ultralow voltage, OTFT-based sensor for label-free DNA detection, Adv. Mater. 25 (2013) 103–107.
[16] A. Caboni, E. Orgiu, E. Scavetta, M. Barbaro, A. Bonfiglio, Organic-based sensor for chemical detection in aqueous solution, App. Phys. Lett. 95 (2009) 123304.
[17] M. Demelas, S. Lai, G. Casula, E. Scavetta, M. Barbaro, A. Bonfiglio, An organic, charge-modulated field effect transistor for DNA detection, Sens. Actuators B-Chem. 171–172 (2012) 198–203.
[18] M. Barbaro, A. Caboni, D. Loi, S. Lai, A. Homsy, P.D. Van Der Wal, N.F. De Rooij, Label-free, direct DNA detection by means of a standard CMOS electronic chip, Sens. Actuators B-Chem. 171–172 (2012) 148–154.
[19] M. Barbaro, A. Bonfiglio, L. Raffo, A charge-Modulated FET for detection of biomolecular processes: conception, modeling, and simulation, IEEE Trans. Electron Devices 53 (2006) 158–166.
[20] M. Demelas, S. Lai, A. Spanu, S. Martinoia, P. Cosseddu, M. Barbaro, A. Bonfiglio, Charge sensing by organic charge-modulated field-effect transistors: application to the detection of bio-related effects, J. Mater. Chem. B 1 (2015) 3811–3819.
[21] S. Lai, P. Cosseddu, G.C. Gazzadi, M. Barbaro, A. Bonfiglio, Towards high frequency performances of ultra-low voltage OTFTs: combining self-alignment and hybrid, nanosized dielectrics, Org. Electron. 14 (2013) 754–761.
[22] T.M. Herne, M.J. Tarlov, Characterization of DNA probes immobilized on gold surfaces, J. Am. Chem. Soc. 119 (1997) 8916–8920.
[23] S. Lai, M. Barbaro, A. Bonfiglio, The role of polarization-induced reorientation of DNA strands on organic field-effect transistor-based biosensors sensitivity at high ionic strength, App. Phys. Lett. 107 (2015) 103301.
[24] B. Cai, S. Wang, L. Huang, Y. Ning, Z. Zhang, G.-J. Zhang, Ultrasensitive label-free detection of PNA-DNA hybridization by reduced graphene oxide field-effect transistor biosensor, ACS Nano 8 (2014) 2632–2638.
[25] T.Y. Chen, P.T. Loan, C.L. Hsu, Y.H. Lee, J. Tse-Wei Wang, K.H. Wei, C.T. Lin, L.J. Li, Label-free detection of DNA hybridization using transistors based on CVD grown graphene, Biosens. Bioelectron. 41 (2013) 103–109.
[26] A. Halperin, A. Buhot, E.B. Zhulina, Sensitivity specificity, and the hybridization isotherms of DNA chips, Biophys. J. 86 (2004) 718–730.

Biographies

Stefano Lai obtained magna cum laude the M.Sc. Degree in Electronics in 2010. He joined the Department of Electrical and Electronic Engineering as Ph.D. student in 2011. He received the Ph.D. in Electronics and Computer Science in 2014. Since 2014, he is a Postdoctoral research fellow in the same Department. His research interests involve the development, fabrication and characterization of field-effect transistor based devices for sensing applications, with a particular focus on biosensors in CMOS and organic technology.

Massimo Barbaro received the M.Sc. (1997) and Ph.D. (2001) degrees in Electronic Engineering from the University of Cagliari, Italy. In 2002 he joined the University of Cagliari, as Assistant Professor in the field of analog microelectronics. His current research interests are the design and realization of CMOS imagers with computational capabilities, CMOS and organic biosensors, implantable neural interfaces. He has published more than 30 papers and holds 2 international patents.

Annalisa Bonfiglio was born in 1966. She received the degree in Physics from the University of Genoa, Italy in 1991 and the Ph.D. degree in Bioengineering from the Polytechnical School of Milan, Italy in 1996. In 1996 she joined the Department of Electrical and Electronic Engineering, University of Cagliari, as an Assistant Professor in the field of Electronic Devices. Since 2004 she is an Associate Professor of Electronics at the same University. Her current research interests are in the field of organic electronics, with a particular focus on the applications to sensors and E-textiles